The multifractal character of the electronic states in disordered two-dimensional systems

1995 J. Phys.: Condens. Matter 7 5549

(http://iopscience.iop.org/0953-8984/7/28/012)

J. Phys.: Condens. Matter 7 (1995) 5549–5565. Printed in the UK

The multifractal character of the electronic states in disordered two-dimensional systems

Nacir Tit†‡ and Michael Schreiber§

† International Centre for Theoretical Physics, PO Box 586, 34100 Trieste, Italy

‡ Physics Department, United Arab Emirates University, PO Box 17551, Al-Ain, United Arab Emirates||

§ Institut für Physik, Technische Universität Chemnitz–Zwickau, D-09107 Chemnitz, Germany

Received 7 December 1994, in final form 3 May 1995

Abstract. The nature of electronic states in disordered two-dimensional (2D) systems is investigated. With this aim, we present our calculations of both density of states and d.c. conductivity for square lattices modelling the Anderson Hamiltonian with on-site energies randomly chosen from a box distribution of width W. For weak disorder (W), the eigenfunctions calculated by means of the Lanczos diagonalization algorithm display spatial fluctuations reflecting their (multi)fractal behaviour. For increasing disorder the observed increase of the curdling of the wavefunction reflects its stronger localization. However, as a function of energy, the eigenstates at energy $|E|/V \simeq 1.5$ are found to be the least localized over the band. Our d.c. conductivity results suggest a critical fractal dimension $d_c^* = 1.48 \pm 0.17$ to discriminate between the exponentially and the power-law-localized states. Consequences of the localization for transport properties are also discussed.

1. Introduction

Since the formulation of the one-parameter scaling hypothesis of localization by Abrahams *et al* [1], the subject of Anderson localization has attracted increasing interest with a rapid development of new theoretical and experimental approaches. The scaling hypothesis [1] predicts a metal–insulator transition (MIT) to occur only in 3D systems and an exponential localization of all eigenstates (with the localization length λ) for any arbitrary small but finite disorder in two- and one-dimensional systems. However, the latter behaviour is very difficult to detect if the corresponding localization length λ is macroscopically large as is the case when diminishing the strength of disorder in 2D systems. Thus, here, it appears questionable [2–4] whether the concept of exponentially localized states is reasonable in the weak-disorder limit. In this respect, Kaveh and Mott [5, 6] have argued for a two-parameter scaling theory giving a well defined 'pseudomobility edge' separating two types of localized state—the exponentially localized states away from the band centre and algebraically (power-law-) localized states towards midband. This is in agreement with the experimentally determined β function of Davies *et al* [7]. Both of the above characteristics can be accommodated, however, if one associates an exponential envelope function $e^{-r/\lambda}$ with large λ with the power-law-localized state $\Psi \sim r^{-\alpha}$. Then the power-law decay would govern the character of the wavefunction at small distances while the asymptotic exponential behaviour dominates at large length scales. Hence this exponential factor would have the side-effect of producing

|| Present address.

0953-8984/95/285549+17$19.50

a normalizable wavefunction. In fact it becomes a general belief [8, 9] that homogeneously extended states (and correspondingly a mobility edge) exist only in 3D systems for weak disorder and in 2D systems with inclusion of a strong perpendicular magnetic field.

There has always been a problem of how to characterize the wavefunctions in a weakly disordered system. One characterization is the localization length λ, which describes the exponential decay of the localized state. Another is the correlation length ξ, which describes the spatial extent of the correlations in the amplitude fluctuations of the extended state. On the other hand, to describe the spatial extent of the localized wavefunction by an exponential decay length has suffered not only from the difficulty of computing reasonably large systems (of the order of λ) but also from strong spatial fluctuations of the amplitude of the wavefunction which correspond to the fluctuations of the extended wavefunction. These fluctuations are therefore a characteristic feature of the wavefunction in a disordered system and have been believed to mask—at least on small length scales—the homogeneously extended or the exponentially localized behaviour. At the mobility edge, in 3D systems, these fluctuations occur on all length scales larger than the lattice spacing. This has led to the suggestion that they display self-similar fluctuations (i.e., they are fractal entities). This idea was first suggested by Aoki [9] and was corroborated by numerical investigations [10, 11]. Furthermore, the calculation of the generalized fractal dimensions and the singularity spectrum of the fractal measure [11] have confirmed the multifractal behaviour of the wavefunctions at the mobility edge in 3D systems. This yields a comprehensive picture to describe the continuous transition from exponentially localized to homogeneously extended states. In particular, as the traditional assumption of exponential spatial decay of the localized wavefunctions may not reflect the most significant features, the multifractal description becomes necessary for their correct characterization.

The fractal behaviour of the eigenstates has been observed not only at the mobility edge but more generally also for the short-range fluctuations of the wavefunctions in disordered systems up to length scales of the order of localization length λ and the coherence length ξ of localized and extended states respectively [10, 12]. This was demonstrated for extended states [12, 13] as well as for localized states in 1D [14] and 2D [15, 16]. In this context, we would like to emphasize that there still exists some controversy about the multifractality of localized states and in general all states away from criticality. However, the task of analysing this issue has always been complicated by the obvious difficulty of dealing with finite-size numerical realizations. This has limited several authors to study mainly one-dimensional systems. For instance, Pietronero *et al* [17] have shown in their multifractal analysis of the weakly disordered 1D Anderson wavefunctions the absence of self-similarity for the space fluctuations and multifractality for the disorder fluctuations in full analogy with the properties of the multiplicative random walk. Following the same analysis but using an incommensurate potential (that yields a transition for all states from extended to localized as a function of the amplitude of this potential), Siebesma and Pietronero [18] have shown the multifractality not only at the critical point but also for extended and localized wavefunctions up to the correlation length and localization length respectively. This situation is analogous to 3D systems and should provide indirect support to the multifractality of the states away from the mobility edge. On the other hand, Mato and Caro [14] have calculated the generalized dimension $D(q)$ and the singularity spectrum for 1D weakly disordered wavefunctions and have shown their multifractal character. This, indeed, contradicts the view [19] that multifractality is associated with the critical phenomenon of crossing the mobility edge in $(2+\epsilon)$-dimensional systems. Roman [20] also attempted to discover the multifractality of localized 1D wavefunctions but concluded from his multifractal analysis that, in spite of the spatial fluctuations, a 1D wavefunction is essentially a uniform object.

The same author claimed [21] the same view using the partition function $\xi_q(L)$. However, since it is a delicate task to determine the mass exponents $\tau(q)$ of $\xi_q(L)$ from the doubly logarithmic plots of $\xi_q(L) \sim L^{-\tau(q)}$, Schreiber and Grussbach [22] studied the singularity spectrum $f(\alpha)$ which can be determined with sufficient accuracy in terms of q. Their singularity spectrum is typical for multifractal entities. The mass exponent $\tau(q)$ was obtained by means of Legendre transformation of $f(\alpha)$. This latter quantity also proves a multifractal character. Hence, it is not surprising that 2D wavefunctions are considered to have multifractal properties in this paper.

The multifractal behaviour of weakly localized wavefunctions was corroborated by the calculation of the singularity spectrum $f(\alpha)$ for 1D [14, 22] and 2D [23]. Furthermore, we should note the fundamental difference between 1D and 2D disordered wavefunctions. In the weak-disorder limit, both wavefunctions can be expanded in terms of Bloch functions. Within the one-band approximation, the 1D wavefunction consists of two Bloch functions of wavevectors $k = \pm\sqrt{2mE/\hbar^2}$ with small admixture of other Bloch functions close in energy. This admixture reflects the influence of the weak disorder. On the other hand, the 2D wavefunction consists of a linear combination of a much bigger number of Bloch functions possessing approximately the same energy, $E \simeq (\hbar^2/2m)(k_x^2 + k_y^2)$. As a consequence, fluctuations appear at all length scales, because small and large wavevectors contribute. Moreover, it is important to note that the localization length in 2D can be macroscopically large even for disorders, W, which are not very small (see table 1). This, in fact, suggests the possibility of multifractality on length scales up to this macroscopically large localization length. Of course, the question which remains is to understand what happens in the thermodynamic limit. Probably, one gets an exponentially localized wavefunction which shows multifractal behaviour only on small scales. Lastly, we note that the singularity spectrum of the 2D wavefunction [23] is more symmetric than that of the 1D wavefunction [22]. The former is more like a parabola in shape, reflecting the fact that the multifractal character of the fluctuations is more prominent because the localization length is larger and therefore the range of length scales on which the multifractality manifests itself is larger.

Table 1. The localization lengths and corresponding fractal dimensions at the midband ($E = 0$) for a square lattice, interpolated from figures 5(a) and 5(b) respectively for various disorder strengths W used in our present work.

W/V	λ(ESZ) [42]	λ(SO) [43]	λ(MK) [41]	$d^*(E = 0)$ [16]
1	$>7 \times 10^8$	$>10^6$	$>10^6$	> 1.85
1.8	$>7 \times 10^8$	$>10^6$	$>10^6$	1.85
2	6.34×10^8	$>10^6$	7.99×10^5	1.84
2.6	7.56×10^5	2.18×10^5	2.6×10^4	1.80
3.6	4328.0	2911.4	1137.7	1.71
4	1123.0	1027.7	481.0	1.70
5.2	125.8	137.8	82.0	1.53
5.5	94.1	88.0	58.6	1.48
6	41.3	51.3	37.5	1.41
6.2	37.7	43.9	32.8	1.37
6.7	28.5	28.6	22.9	1.31
7.3	20.4	18.9	16.3	1.20
8	10.9	12.5	11.1	1.08
10.4	5.0	5.5	4.9	0.67
16	1.7	2.0	1.9	—

In this respect, the fractal character of the wavefunction was proposed [10, 12] as a new

method for finding the mobility edge. Later, when the multifractal characteristics became appreciated, a particular singularity spectrum was assumed as a signature of the metal–insulator transition [11, 13]. This was corroborated by the investigation of various systems [24].

The transport properties are, of course, drastically influenced by the (multi)fractal behaviour. The question which is raised here is which fractal dimension (among the set of multifractal dimensions) is significant for the description of the transport properties. Several authors [25, 26] have suggested the correlation dimension (this point is discussed further below).

This latter idea was numerically exploited by several authors, determining the fractal dimension from either the density–density correlation function [10] or, equivalently, the participation number [12], or from the amplitude of the wavefunction [27]. We note that the correlation dimension should coincide with the fractal dimension determined from the participation ratio calculation [28]. Calculating the fractal dimension d^* from the participation number in 3D systems for various disorder strengths [29], it was possible to estimate a critical fractal dimension $d_c^* = 1.6 \pm 0.1$ corresponding to the metal–insulator transition (i.e., eigenfunctions which yield a lower fractal dimension are localized and those which yield a higher one are extended). From this dimension, the trajectory of the mobility edge in the disorder–energy (W–E) diagram could be derived. This calculation also confirms that the transition between the extended states, through the fractal regime, to the strongly localized states is smooth. The result $d^* = 1.6$ corresponds to a critical disorder $W_c \simeq 21$ (which is reasonable for the employed Gaussian distribution of the diagonal elements of the Anderson Hamiltonian) and yields a mobility edge trajectory in good agreement with the results of the finite-size scaling approach [30].

It is interesting to note the difference in the physics and dimensionality between the terms fractal and fracton. First of all, fractals can be classified as deterministic or random depending on whether the self-similarity is exact or considered as a stochastic property. For instance, diffusion-limited aggregation (DLA), percolating networks, Ising spin systems and fluctuations of the amplitude of the wavefunction in disordered systems present some typical examples of random fractals. The fractal dimension, d_f, describes how the mass of the geometrical object depends on its length scales. In more general terms, the fractal dimension reflects the scaling of the moments of the mass. In our investigation, we concentrate on the fractal dimension d^* of the participation ratio which coincides with the fractal dimension of the second moment of the mass. It can be shown [28] that in the present model this dimension d^* is also equivalent to the fractal dimension of the density–density correlation [10]. That is not equivalent, however, to the fractal dimension of the mass but is a consequence of the multifractality [11]. Only for a homogeneous fractal, not for a multifractal, would these values coincide. In contrast the fracton dimension $\tilde{d}$ characterizes anomalous diffusion on the fractal substrate. This fracton dimension is connected to d_f by the relation [31] $\tilde{d} = 2d_f/(2+\theta)$, where θ is the exponent giving the dependence of the diffusion constant on distance. The term 'fracton', in fact, denotes a localized vibrational mode peculiar to a fractal structure, coined by Alexander and Orbach [31]. These excitations exist not only for vibrational systems but also for, e.g., dilute magnets [32]. Moreover, Alexander and Orbach [31] noted that the fracton dimension $\tilde{d}$ for percolating networks was numerically close to the mean-field value $\tilde{d} \approx \frac{4}{3}$ for any Euclidean dimension $d \geqslant 2$. This came to be known as the Alexander–Orbach conjecture. Immediately after this work Rammal and Toulouse [33] developed an analogous scaling method (based on the scaling theory of localization of Abrahams *et al* [1]) to calculate the vibrational density of states (DOS) and the mean number of sites visited by a random walker

on a fractal network as substrate. These latter quantities were both shown to be characterized by the same fracton dimension $\tilde{d}$. Thus $\tilde{d}$ reflects the scaling of the spectral density of the fracton vibrations. This is why $\tilde{d}$ is also called the spectral dimension. This notion of the fracton was further corroborated by the large-scale computation of Yakubo and Nakayama [34], who performed calculations of the DOS for 2D and 3D percolating networks of size of the order of $N \sim 10^5$ sites. Their results showed that the frequency dependence of the DOS can be characterized by two regimes. (i) In the high-frequency regime ($\omega \gg \omega_c$), the DOS is closely proportional to $\omega^{1/3}$ and independent of the Euclidean dimensionality. The crossover frequency ω_c corresponds to the mode of wavelength Λ equal to the percolating correlation length 'l'. (ii) In the low-frequency regime $\omega \ll \omega_c$, however, the DOS is given by the conventional Debye law $D(\omega) \propto \omega^{d-1}$, where d is the Euclidean dimension of the lattice, whereas $D(\omega) \propto \omega^{\tilde{d}-1}$ for $\omega \gg \omega_c$ with $\tilde{d} = \frac{4}{3}$. This work, hence, has numerically supported the Alexander–Orbach conjecture and shown that vibrational excitations, whose wavelength Λ is smaller than the percolation correlation length l and which therefore exist in the high-frequency regime, are localized and called 'fractons'. Note that as soon as Λ becomes longer than l, the vibration exhibits a transition from a fracton to a phonon (delocalized vibrational mode). Lastly, we briefly summarize that the term 'fracton' introduced by Alexander and Orbach [31] stands for an anomalous diffusion on a percolating fractal network, and has been theoretically predicted through both scaling arguments [31, 33, 35] and large-scale simulations [34], and has been experimentally observed using both light [36] and inelastic neutron [37] scattering measurements. Moreover, as the fracton is supported by a fractal network one always expects that $\tilde{d} < d_f < d$. For the Anderson model on a regular lattice, however, the fractal dimension d_f is equal to the Euclidean dimension d. In the rest of the paper, we discuss therefore the most important generalized dimension d^* of the multifractal wavefunction. As mentioned above, d^* is obtained from the participation ratio calculation [16], and is equivalent to the dimension calculated from the density in [10].

The scope of this paper, however, is to readdress the question of searching for the critical fractal dimension d_c^* (in absence of magnetic field), which can discriminate between the exponentially and the power-law-localized states in 2D systems. For this task, we employ the Anderson Hamiltonian with on-site energies taken from the box distribution. We calculated both the density of states and the d.c. conductivity, based on the Kubo–Greenwood formula, versus energy and disorder (W). Our calculations were performed on square lattices containing numbers of sites ranging from 300 to 10 000 sites. The d.c. conductivity results are used to search for the critical disorder W_c, above which the midband states become exponentially localized. (Here our conductivity reference for localization is taken to be Mott's minimum metallic conductivity, σ_{min}.) We used the obtained W_c of the largest sample (of size $N = 100 \times 100$ sites) and by interpolating the results of fractal dimension $d^*(E)$ of [16], we estimated a critical fractal dimension $d_c^* = 1.48 \pm 0.17$ to separate between the exponentially and the power-law-localized states.

In the next section we describe the model and the calculations of both density of states and d.c. conductivity. In section 3, we present and discuss our results. The last section summarizes our conclusions.

2. Computational details

Our investigation is based on the Anderson model, commonly used to study the localization of the wavefunctions in disordered systems. In site representation, the one-electron

Hamiltonian is given by

$$H = \sum_n |n\rangle \epsilon_n \langle n| + \sum_{\langle n,m \rangle} |n\rangle V_{nm} \langle m| \tag{1}$$

where the on-site energies ϵ_n are randomly chosen from a box distribution of width W, reflecting the strength of the disorder. The transfer integrals $V_{nm} = V$ are restricted to nearest-neighbour sites n and m only, as indicated by the brackets $\langle\ \rangle$, and define the energy scale ($V = 1$). At vanishing disorder, one expects the energy spectrum to extend from $-\nu$ to ν, where ν is the number of nearest neighbours.

The energy spectrum of the Hamiltonian (1) and the corresponding wavefunctions are calculated using a direct diagonalization procedure based on the Lanczos algorithm [38]. This diagonalization method is known to be very efficient for large sparse matrices. We applied this method to the Hamiltonian (1) for square lattices with periodic boundary conditions.

We used the obtained energy spectrum to calculate the density of states:

$$N(E) = \sum_\mu \delta(E - E_\mu) \tag{2}$$

where μ labels the eigenstates of the Hamiltonian. Both eigenvalues and eigenvectors of the Hamiltonian are needed to calculate the d.c. conductivity, which is given [39] by the Kubo–Greenwood formula, for a noninteracting electron system within the linear response theory at $T = 0$ K (with $E_F = E$)

$$\sigma(E) = \frac{2\pi\hbar e^2}{m^2\Omega} \sum_{\mu,\nu} |\langle \mu | P^x | \nu \rangle|^2 \, \delta(E - E_\mu)\, \delta(E - E_\nu). \tag{3}$$

Here the polarization is taken in the direction of the x-axis, μ and ν label eigenstates, P^x is the momentum operator ($P^x/m = -(\mathrm{i}/\hbar)[x, H]$), Ω is the volume of the sample, and H is the Hamiltonian (1) of the system. We note that we have performed ensemble averaging over different realizations of the random potentials for both quantities (2) and (3). The number of realizations varies from 256 to eight realizations (per half band) corresponding to the smallest ($N = 300$ sites) and largest ($N = 10\,000$ sites) samples, respectively.

3. Results and discussion

We first display in figure 1 the obtained probability amplitudes of (sums of) eigenstates of the Hamiltonian (1) on square lattices of size 50×50 sites for various parameter combinations of energy and disorder. These figures (1(a)–(f)) are obtained by averaging over the mentioned realizations and over all eigenstates in an energy window of $\Delta E = 0.1$. Hence each of them represents a wave packet of eigenfunctions. In all these density plots we show only sites for which the amplitudes are larger than the average ($1/\sqrt{N}$). The darker the square dots the higher the amplitudes of the wavefunctions are. The white regions are areas of weak probability density. The figures 1(a)–(f) demonstrate the fragmentation of the probability density of the wave packets. This is a behaviour typical for fractal entities. However, in displaying these figures we are not attempting to prove the (multi)fractality because it is out of the scope of this paper and to do this one should either employ the original definition of Hausdorff measure or follow a multifractal analysis similar to the one given in [40].

Figure 1(a) corresponds to the smallest energy and smallest disorder ($E = 0$, $W = 1.8$). Typical curdling of the amplitude of the wavefunction can clearly be seen and would indicate the fractal entities as described above. Figures 1(b) and 1(c) display the eigenstates of higher

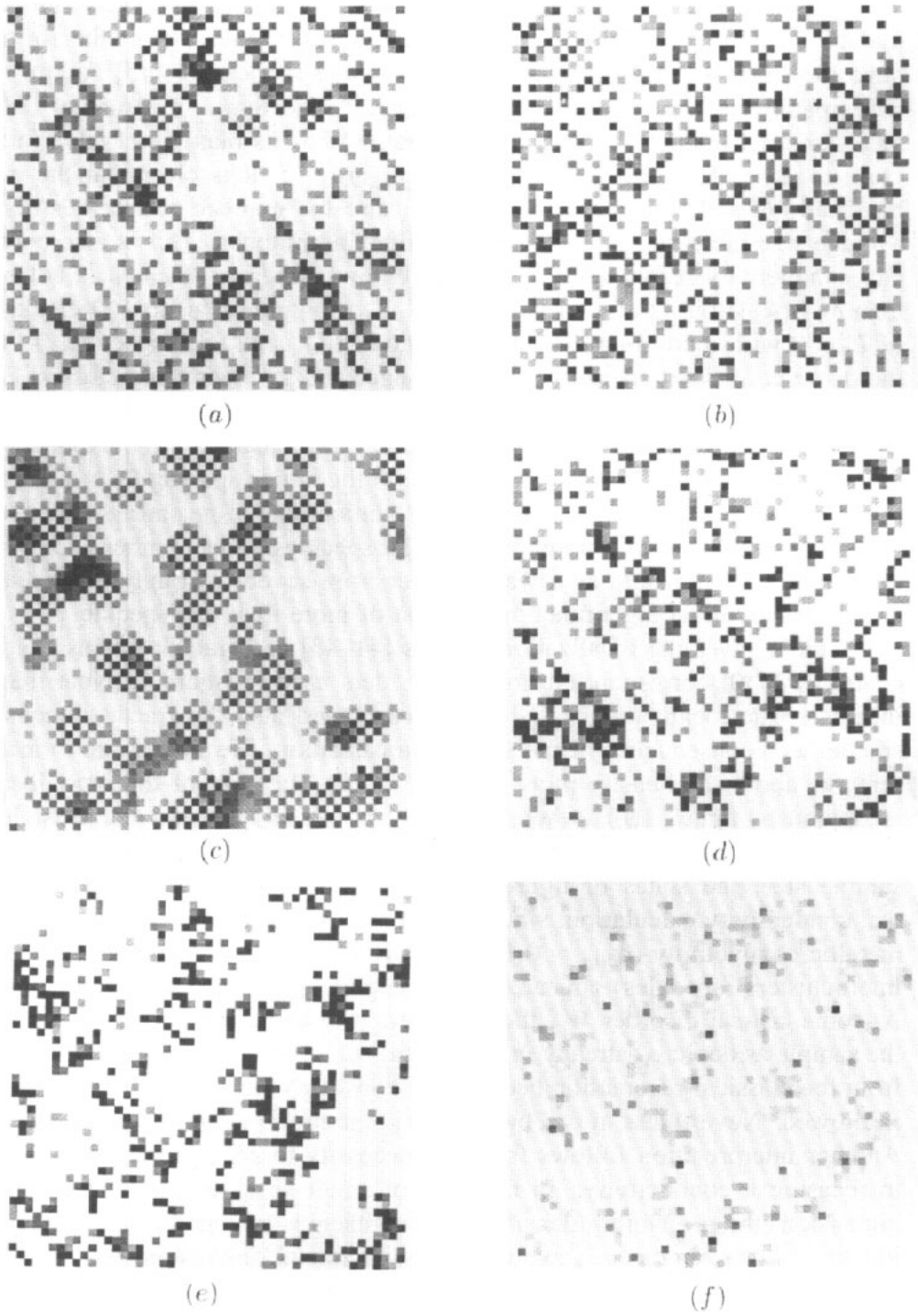

Figure 1. Probability amplitude of wave packets on a square lattice of size $N = 50 \times 50$ sites. We start from (a) $E = 0$, $W = 1.8$ then the energy is increased to (b) $E = 2$ and (c) $E = 4$. Then we restart from (a) and the disorder is increased to (d) $W = 6.2$, (e) $W = 10.4$ and (f) $W = 16$. The ensemble averaging in all these figures includes 12 realizations. Every site with an amplitude larger than the average ($|e_{in}| > N^{-1/2}$) is shown. Four different grey levels ($j = 0, 1, 2, 3$) are used to distinguish whether $e_{in}^2 > 2^j/N$.

energy ($E = 2$ and $E = 4$, respectively) but for the same disorder, $W = 1.8$, as in figure 1(a). While one expects more and more localization to occur, it seems that the eigenstate

of energy $E = 2$ is more homogeneously spread and, therefore, more delocalized than that of $E = 0$. From this observation only, one would expect the former eigenstate to have the highest participation number (which is a measure [15] for the number of sites participating in a given eigenstate at energy E and thus a measure of delocalization). In fact, our d.c. conductivity (see figure 4 below) has its maximum value (at about $E = 1.5$) close to $E \simeq 2$ when $W = 1.8$. From figure 1(c) it is clear that the eigenstates at the band tail ($E = 4$) are more localized because the number of speckles decreases but their average size increases as well as the maximal amplitudes. This is also corroborated by our d.c. conductivity results (see figure 4(a) below), where $\sigma(E = 4)$ is not only much lower than $\sigma(E < 4)$ but is also of the order of σ_{min}. Figures 1(d) to 1(f) display the eigenstates of $E = 0$ with increasing disorder ($W = 6.2$, 10.4 and 16, respectively). When increasing the disorder at fixed energy ($E = 0$) stronger and stronger microclusters (speckles) appear with increasingly broad valleys in between and the wavefunction appears more and more localized. Figure 1(f) displays strong localization; analysing the exponential decay of this function yields a localization length equal to the lattice spacing ($\lambda \approx 1$ site). It is important to note, however, that in spite of this localization length the state is not restricted to mainly one site, but consists of a number of similar speckles. This number is only partly due to the construction of the state as a wave packet from several strongly localized eigenfunctions. Even the individual eigenfunctions consist of more than one speckle.

Table 1 gives the localization lengths [41–43] and fractal dimensions [16] at the band centre ($E = 0$) corresponding to the disorders used in figure 1. Note that as the disorder increases, the localization length λ decreases and also the fractal dimension d^* becomes smaller as a consequence of the stronger localization. We would like to make the following remarks about the density plots of figure 1. (i) The case of the most localized eigenstate is obviously figure 1(f) (where $E = 0$ and $W = 16$) and the least localized state is the one of figure 1(b) (where $E = 2$ and $W = 1.8$). (ii) With respect to this finite sample size, the states of figures 1(c), 1(e) and 1(f) are localized as confirmed in our d.c. conductivity calculation, where their corresponding $\sigma(E)$ is less than Mott's minimum metallic conductivity ($\sigma_{min} \sim 0.1e^2/\hbar$). (iii) When decreasing the disorder, more and more microclusters (speckles) appear, which support a significant amount of the wavefunction. At some critical disorder W_c, these clusters join and allow a percolation-like path through the sample as depicted already in figure 1(a). Of course, it is understood that this is different from the classical percolation because we consider here a quantum system where tunnelling is allowed. Neverthless, it can bring a vivid picture of localization of the electronic density. Another interpretation follows from the necessity to apply contacts to the sample in order to measure a conductivity: in the case of small speckles (or, equivalently, small fractal dimension) the probability density at the contacts is too small to sustain the current. If one imagines, for example, a wavefunction with fractal dimension two on a 3D finite lattice, then the effective contact is of fractal dimension one if the entire sides of the sample cube are contacted.

Now, we discuss our d.c. conductivity results. In figure 2, we show the results of both density of states (DOS) (in units of 1 eV^{-1}) and d.c. conductivity $\sigma(E)$ (in units of $e^2/\hbar$) which is the same as conductance in 2D for a sample of size 20×20 sites with disorders ranging from $W = 1$ to 16. The plots are shown for half the band $E \geqslant 0$ to obtain better ensemble averaging by taking the mean of the two band sides. We note the following points. (i) First, one clearly sees the expected decrease of conductivity with increasing disorder (W). Since the averaging over disorder includes about 256 realizations of the random potentials, the displayed conductance fluctuations are presumed to be mainly due to the finite-size effects. (ii) For disorders $W \leqslant 4$, overall the conductivity follows

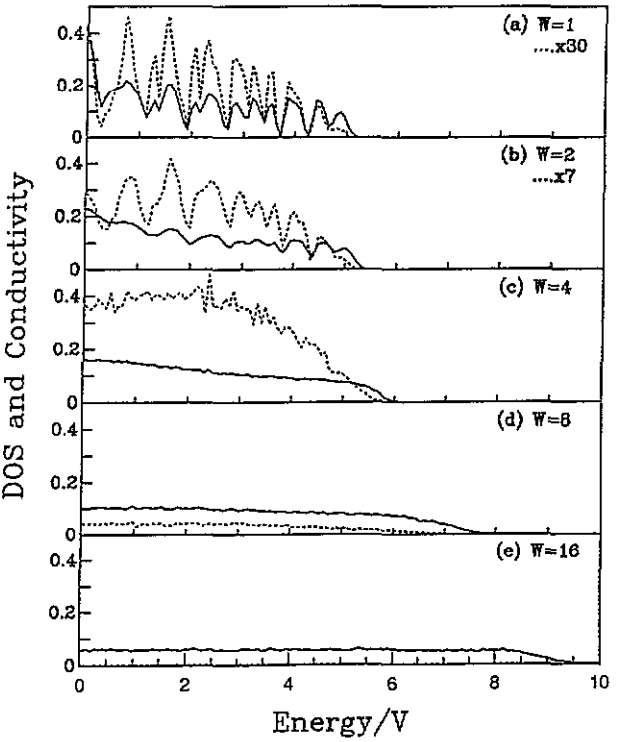

Figure 2. DOS (solid curves) and d.c. conductivity (dotted curves) for a sample of $N = 20 \times 20$ sites with the disorders (a) $W = 1$, (b) $W = 2$, (c) $W = 4$, (d) $W = 8$ and (e) $W = 16$. The scale is in units of 1 eV^{-1} for the DOS and in units of $e^2/\hbar$ for the conductivity. The ensemble averaging comprises 256 realizations. Note that $\sigma(E)$ in (a) and (b) is reduced by a factor of 30 and seven, respectively.

the density of states profile, but vanishes already for energies smaller than the band tails, where the DOS remains substantial. This may suggest a 'pseudomobility edge' separating two types of state: the inner states towards midband are more conducting and therefore less localized than the states on the outer sides of the 'pseudomobility' edges. (iii) For disorders $W \geqslant 8$, however, it seems that all states are localized as long as $\sigma(E)$ is less than σ_{min}. This is also consistent with the estimated localization lengths listed in table 1, namely $\lambda < L$.

Similar observations can be made for larger samples of sizes 30×30 and 50×50 sites from the results displayed in figures 3 and 4, respectively. These figures may give an idea about the scaling of conductance. For weak disorders ($W = 1.8, 2.6$ and 3.6), for which the localization lengths are much bigger than these sample sizes (see table 1), the results suggest that the conductance falls monotonically with increasing lattice size. For higher disorder ($W \geqslant 6.7$), however, the results suggest that all the states are strongly localized as $\sigma(E) < \sigma_{min}$ over all the band. This latter is consistent with the small values of localization lengths of table 1. Of course, a definite proof of the strong localization of the full band for any disorder requires much larger samples and this was beyond our limited computational means. Lastly we note that the displayed curves in figures 3(e) and 4(e) correspond to two different disorders $W = 6.7$ and 6.2 respectively. These disorder values yield $\sigma(0) \sim \sigma_{min}$. This seems reasonable as larger samples require smaller critical disorder W_c to make all

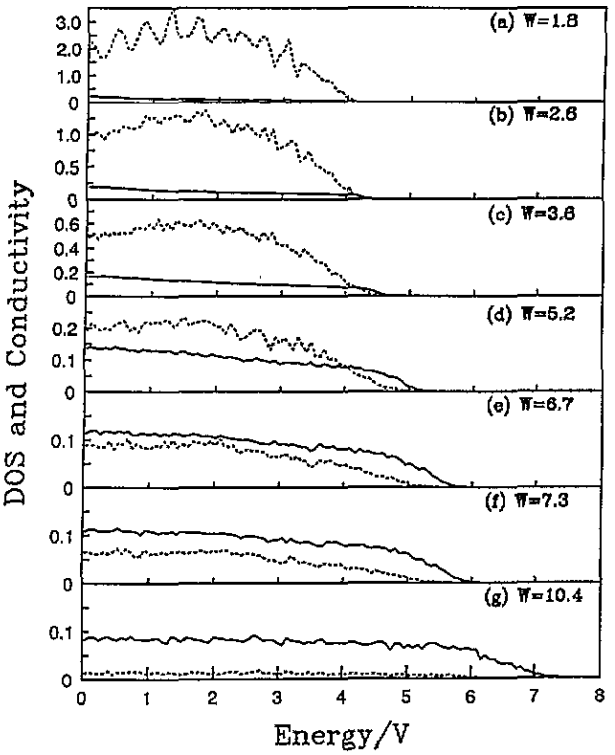

Figure 3. Same as figure 2 but for a sample of size $N = 30 \times 30$ sites with disorders (a) $W = 1.8$, (b) $W = 2.6$, (c) $W = 3.6$, (d) $W = 5.2$, (e) $W = 6.7$, (f) $W = 7.3$, (g) $W = 10.4$. The ensemble averaging includes 56 realizations.

their states strongly localized when the localization length λ becomes smaller than L.

For completeness, we have compiled in figure 5(a) some available estimations in the literature of the localization lengths at the band centre $\lambda(E = 0)$ versus disorder W. In this figure 5(a), the data shown in open circles (○) and crosses (×) have been obtained from the calculation of transmission probability using the strip (bar) method in [43] and [41] respectively. However the data shown in triangles (△) are obtained from the potential well analogy method [42]. In figure 5(b), we display the fractal dimension d^* at the midband ($E = 0$) for various disorders reported in [16] from participation number calculations.

The next point we would like to discuss is what will happen when the sample size is scaled only in one (x or y) direction. For this, we fixed the disorder $W = 6$. Figure 6 shows the scaling of conductance in the x direction for samples of sizes varying from 10×30 to 70×30 sites. To get a clearer idea, we have presented the calculations of $\sigma(E)$ on an expanded scale for only three samples in figure 7. Large fluctuations of the conductance as E varies over the band are clearly observed. These are presumed to be partly due to disorder (the universal conductance fluctuation, which is essentially a quantum effect governed by quantum tunnelling and interference) and partly due to the finite-size effects.

Figure 8, however, displays the finite-size scaling of conductivity in the y direction for samples of sizes ranging from 30×10 to 30×70 sites. Similarly, we have drawn the $\sigma(E)$ results in figure 9 on an expanded scale for only three samples. As one might intuitively predict, the conductivity $\sigma(E)$ seems to increase with the growing of the y side of the sample. We again emphasize that the conductivity is calculated in the x direction as

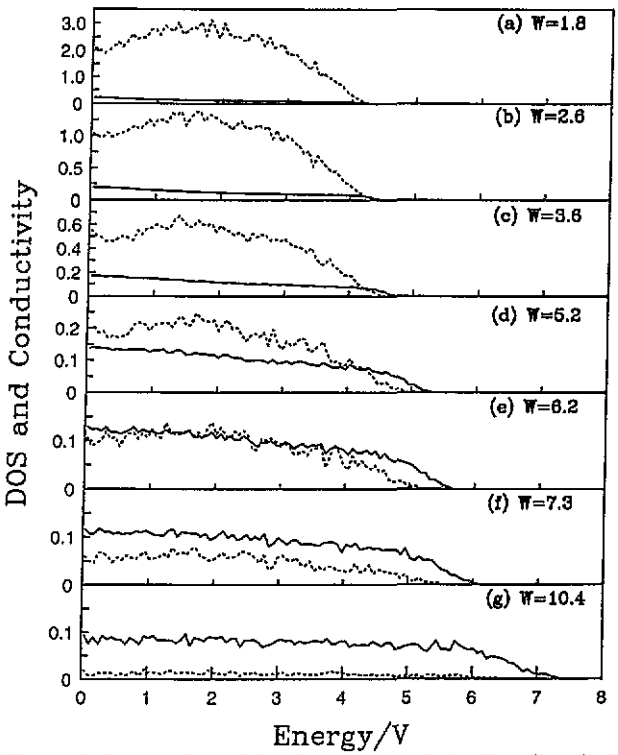

Figure 4. Same as figure 3 but for a sample of size $N = 50 \times 50$ sites. Here, 12 realizations are included in the ensemble averaging. Note that the disorder in (e) is $W = 6.2$, different from that of figure 3(e).

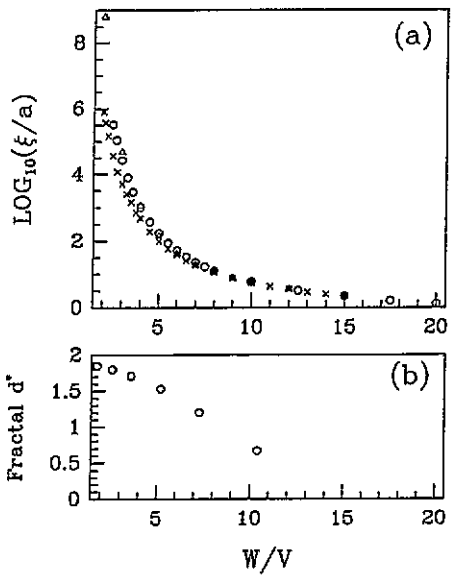

Figure 5. (a) The logarithm of localization length $\lambda(E = 0)$ as a function of disorder W for a square lattice is compiled from three different sources: triangles (△) due to [42], open circles (○) due to [43] and crosses (×) due to [41]. (b) Fractal dimension at band centre $d^*(E = 0)$ due to [16]. Note that the disorder scale in both (a) and (b) starts from $W/V = 1.5$.

explicitly indicated in (3). This growing conductivity with increasing y side sample sizes can be explained by the increase of the number of tunnelling channels or, as mentioned

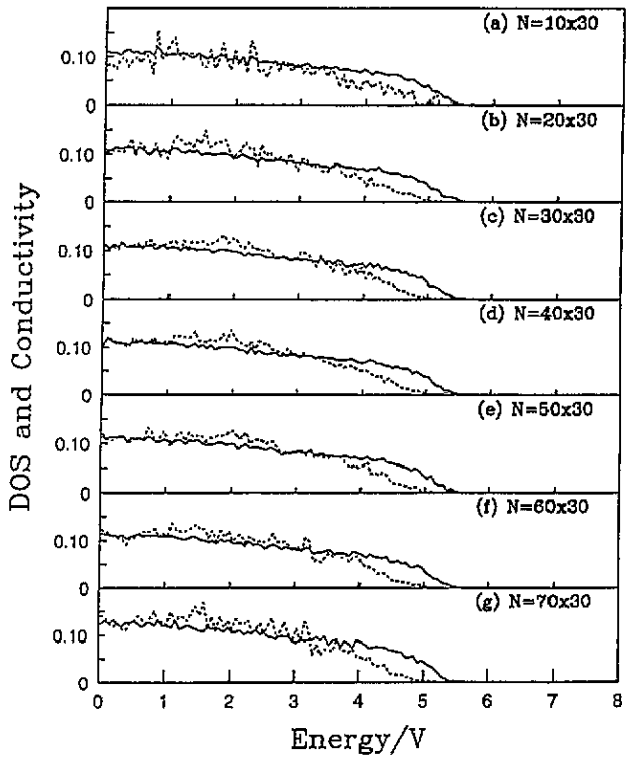

Figure 6. Scaling of conductivity versus the x side of the 2D sample at fixed disorder $W/V = 6$. DOS is shown in solid curves in units of 1 eV^{-1} and conductivity in dotted curves in units of $e^2/\hbar$. The number of realizations used in the ensemble averaging is (a) 130, (b) 84, (c) 56, (d) 42, (e) 34, (f) 26 and (g) 16.

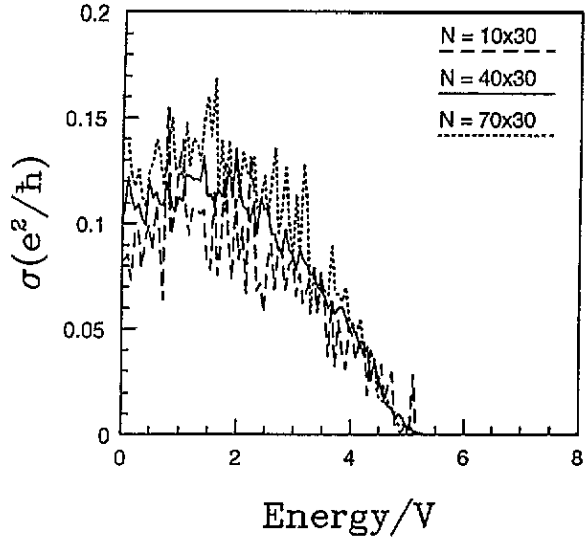

Figure 7. The d.c. conductivity for some of the samples displayed in figure 6.

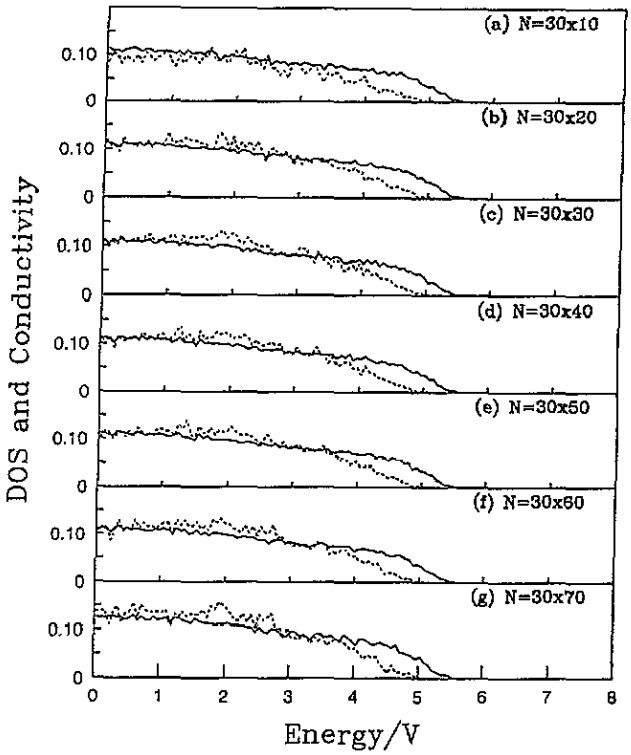

Figure 8. Same as figure 6 but the sample is scaled this time in the y-direction.

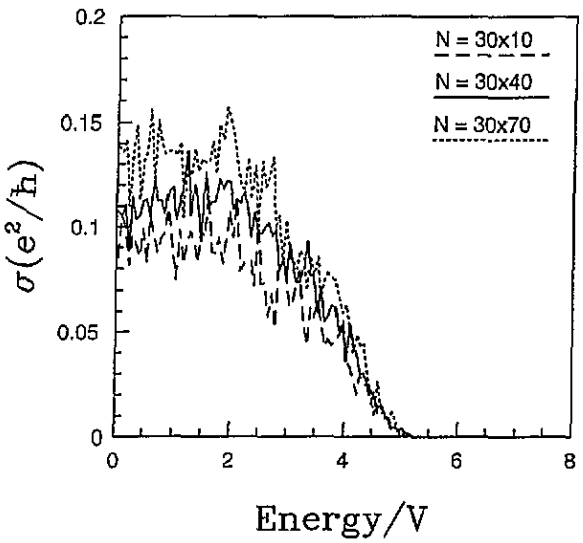

Figure 9. The d.c. conductivity for some of the samples displayed in figure 8.

above, interpreted by the increase of the contact area.

Throughout our discussion of the d.c. conductivity results versus disorder (namely those displayed in figures 2 to 4), the existence of a critical disorder W_c can be inferred depending

on the sample size beyond which all the eigenstates are localized. Our results shown in figures 3 and 4, due to the respective samples of sizes 30×30 and 50×50 sites, have suggested critical disorders $W_c \approx 6.7$ and 6.2 and corresponding critical fractal dimensions $d_c = 1.31$ and 1.37, respectively, according to table 1 and figure 5. The highest estimations of localization lengths (table 1) for these two respective disorders are $\lambda \simeq 28$ and 44 sites, which are smaller than but of the same order as the respective sample sizes. As the conductivity in infinite 2D systems is expected to vanish, one would expect W_c to diminish with increasing sample sizes. In consistency with this, our preliminary d.c. conductivity results on a sample of 100×100 sites at the midband, $\sigma(E = 0)$, suggested a critical disorder of $W_c = 5.5$ corresponding to $\sigma(E = 0) \approx \sigma_{min}$. Again, this is consistent with the fact that the largest estimated localization length, $\lambda \simeq 94$ lattice spacings, is less than L (see table 1). By an interpolation of the results of [16] (see figure 5(b)), we estimated $d_c^* \simeq 1.48$ to correspond to $W_c = 5.5$. For a detailed analysis in this way, even larger systems than previously studied have to be taken into account to estimate the upper bound of d_c^* which is asymptotically reached in infinite systems. The error bar in determining d_c^* is large (of order 0.2) because we cannot determine W_c precisely from the conductivity plots. This error can be explained first as reflecting the continuous transition aspect which makes it difficult to pinpoint the disorder at which σ_{min} is exceeded and second as due to the relatively small sample sizes used in our calculations which means relatively large fluctuations from sample to sample. We took the value of d_c^* from our largest studied sample (of size $N = 100 \times 100$ sites) as an average value with its error bar of $\Delta d_c^* = 0.17$. This estimated critical fractal dimension $d_c^* = 1.48 \pm 0.17$ appears reasonable because, as shown in figure 5(b), the fractal dimension does not increase strongly for even smaller values of W_c which are expected for larger sample sizes as discussed above. Consequently, while the d_c values obtained for the smaller system sizes are definitely too small, we are confident that $d_c^* = 1.48$ is a reasonable estimate. Moreover, this value of d_c^* lies between the fractal dimension, reported by Aoki [27], of the most extended states in a 2D system with strong perpendicular magnetic field, $d^* = 1.57 \pm 0.03$, and the one reported by Ono *et al* [44], $d^* = 1.39$.

Finally, we discuss the effect of localization on the transport properties at finite temperature. In the fractal picture described in this paper, transport between the different speckles in the strong-localization limit takes place by hopping processes, where the areas between the speckles can be associated with effective potential barriers. The behaviour of the conductivity at low temperature is of type $\sigma \sim \exp\left[-(T_0/T)^{\alpha}\right]$ and is characterized by the exponent α. In the regime of strongly localized states, the transport can therefore be described by the variable-range (phonon-assisted) hopping theory [45] which yields the conductivity

$$\sigma \sim \exp\left[-\left(\frac{T_0}{T}\right)^{\frac{1}{d+1}}\right] \tag{4}$$

where the conductivity exponent $\alpha = 1/(d+1)$, for $d > 1$, yields the well known $T^{-1/4}$ law in 3D. We recall that if the Coulomb interactions are important, one gets an exponent $\alpha = \frac{1}{2}$ as predicted by Efros and Shklowskii [46]. In a more recent model [25], the electron is (almost) restricted to move on a sublattice which is fractal over some range of length scales. Associating with this electron a superlocalized wavefunction at the percolation threshold, $|\Psi(r)| \sim \exp\left[-r^{\zeta}\right]$ where ζ is the superlocalization exponent, and neglecting the Coulomb interactions, Deutscher *et al* [25] showed that the hopping conductivity between such states on the fractal behaves as given by the preceding equation with $\alpha = \zeta/(d_f + \zeta)$. Using the Alexander–Orbach conjecture $\tilde{d} = d_f/\zeta = \frac{4}{3}$, the authors of [25] found the superuniversal

result $\alpha = \frac{3}{7}$. This is not very far from the exponent $\frac{1}{2}$ [45] except that Coulomb interactions are absent. This latter model [25] should apply to systems where intercluster tunnelling is negligible such as atomically disordered mixtures and granular materials. At small length scales, however, the electron does not feel that the medium is fractal and for systems without interactions one expects formula (4) to describe the conductivity behaviour.

With decreasing localization (disorder), in our present model, the speckles become closer and closer and more and more speckles of the wave packet belong to a single wavefunction so that the tunnelling becomes easier until finally percolation-like paths through the entire sample are possible supporting the current. In this context we recall that, as transport is usually concerned with a wave packet travelling through the system, we have already taken this into account in our density plots shown in figure 1. We emphasize further that it has been demonstrated [40] that the wave packet also maintains the multifractal behaviour and follows the characteristics of the central single state.

On the supposition that the information dimension, D_1, should be utilized in this localized regime, one obtains a different temperature dependence of the conductivity. The power in the exponent would be larger than $\frac{1}{4}$ in 3D and larger than $\frac{1}{3}$ in 2D systems as suggested by Aoki [27] because D_1 is found [40] to be less than the Euclidean dimension d. Moreover, the dimension D_1 decreases significantly with increasing disorder, yielding a further increase in the exponent of $1/T$ and a diminution in conductivity as a consequence.

In the metallic regime, on the other hand, the conductivity can be related to the density–density correlation function by means of the Kubo formula [44]. Hence, it can be expected that the fractal correlation dimension D_2 ($\equiv d^*$ here) is the significant dimension for the description of transport properties in this regime.

4. Conclusions

The nature of localization of the disordered two-dimensional Anderson eigenfunctions was studied using our density of states and d.c. conductivity calculations. The fractal correlation dimension D_2 ($\equiv d^*$) is suggested to characterize this localization (i.e., to discriminate between the exponentially and power-law-localized states). Using our d.c. conductivity results, the eigenstates of energy $|E|/V \simeq 1.5$ are found to be more delocalized than those at the band centre ($E = 0$) for the studied samples. The d.c. conductivity diminishes with increasing disorder reflecting stronger localization. This could also be observed through the increase of the curdling of the wavefunction in the density plots. The transition from the exponential to power law localization is believed to be continuous.

For a fixed sample size, there exists a critical disorder (W_c) for the exponential localization of all its eigenfunctions. Taking Mott's minimum metallic conductivity as a criterion for the exponential localization, we determined the critical disorders (W_c) for all our studied square lattices. In this respect, our d.c. conductivity results are consistent with the existing localization lengths in the literature. The fractal dimensions corresponding to the W_c values were obtained from the work of [16]. Based on the results of the sample of size 100×100 sites, we estimated a critical fractal dimension $d_c^* = 1.48 \pm 0.17$ to discriminate between the exponentially and power-law-localized states. This fractal (correlation) dimension is expected to be responsible for the conductivity mainly in the metallic regime.

Finally, our d_c^* value should be tested further using larger sample sizes. This together with an attempt to draw the trajectory of the 'pseudomobility edge', separating the exponentially and the power-law localized states, in the disorder–energy (W–E) plane for various sample sizes are considered in our future work.

Acknowledgments

This work was started during the visit of one of us (NT) to the Johannes-Gutenberg-Universität Mainz during the summer of 1993. He is also indebted to Professor Yu Lu for the invitation to visit the International Centre for Theoretical Physics, where this work was completed. The authors thank Dr H Grussbach for his careful reading of the present manuscript.

References

[1] Abrahams E, Anderson P W, Licciardello D C and Ramakrishnan T V 1979 *Phys. Rev. Lett.* **42** 673
[2] Kravtsov V E and Lerner I V 1984 *Solid State Commun.* **52** 593
[3] Kumar N and Jayannavar A M 1986 *J. Phys. C: Solid State Phys.* **19** L85
[4] Altshuler B L, Kravtsov V E and Lerner I V 1988 *Anderson Localization* ed T Ando and H Fukuyama (Berlin: Springer) p 300
[5] Kaveh M 1985 *J. Phys. C: Solid State Phys.* **17** L79
[6] Mott N F and Kaveh M 1985 *Adv. Phys.* 34 329
[7] Davies R, Pepper M, and Kaveh M 1983 *J. Phys. C: Solid State Phys.* **16** L285
[8] See, for instance,
Kramer B, Bergmann G and Bruynseraede Y (ed) 1984 *Localization, Interactions, and Transport Phenomena* (Berlin: Springer)
[9] Aoki H 1983 *J. Phys. C: Solid State Phys.* **16** L205
[10] Soukoulis C M and Economou E N 1984 *Phys. Rev. Lett.* **52** 565
[11] Schreiber M and Grussbach H 1991 *Phys. Rev. Lett.* **67** 607
[12] Schreiber M 1985 *Phys. Rev.* B **31** 6146
[13] Pook W and Janssen M 1991 *Z. Phys.* B **82** 295
[14] Mato G and Caro A 1985 *J. Phys. C: Solid State Phys.* **20** L717
[15] Schreiber M 1985 *J. Phys. C: Solid State Phys.* **18** 2493
[16] Schreiber M 1991 *Localization (IOP Conf. Proc. 108)* ed J T Chalker (London: Institute of Physics and Physical Society) p 65
[17] Pietronero L, Siebesma A P, Tosatti E and Zannetti M 1987 *Phys. Rev.* B **36** 5635
[18] Siebesma A P and Pietronero L 1987 *Europhys. Lett.* 4 597
[19] Castellani C and Peliti L 1986 *J. Phys. A: Math. Gen.* **19** L429
[20] Roman H E 1988 *Phys. Rev.* B **38** 2948
[21] Roman H E 1992 *Phys. Rev. Lett.* **68** 2856
[22] Schreiber M and Grussbach H 1992 *Phys. Rev. Lett.* **68** 2857
[23] Schreiber M and Grussbach H 1992 *Mod. Phys. Lett.* B **6** 851
[24] Grussbach H and Schreiber M 1995 *Phys. Rev.* B **51** 663
[25] Deutscher G, Lévy Y and Souillard B 1987 *Europhys. Lett.* **4** 577
[26] Harris A B and Aharony A 1987 *Europhys. Lett.* 4 1355
[27] Aoki H 1986 *Phys. Rev.* B **33** 7310
[28] Wegner F 1985 *Localization and Metal–Insulator Transitions* ed H Fritzsche and D Adler (New York: Plenum) p 337
[29] Schreiber M 1990 *Physica* A **167** 188
[30] Bulka B, Schreiber M and Kramer B 1987 *Z. Phys.* B **66** 21
[31] Alexander S and Orbach R 1982 *J. Physique Lett.* **43** L625
[32] For an overview, see
Nakayama T, Yakubo K and Orbach R L 1994 *Rev. Mod. Phys.* **66** 381
[33] Rammal R and Toulouse G 1983 *J. Physique Lett.* **44** L13
[34] Yakubo K and Nakayama T 1989 *Phys. Rev.* B **40** 517
[35] Gefen Y, Aharony A and Alexander S 1983 *Phys. Rev. Lett.* **50** 77
[36] Courtens E, Vacher R, Pelous J and Woignier T 1988 *Europhys. Lett.* **6** 245
[37] Vacher R *et al* 1990 *Phys. Rev. Lett.* **65** 1008
[38] Cullum J K and Willoughby R A 1985 *Lanczos Algorithm for Large Eigenvalue Computations. Vol 1: Theory* (Basel: Birkhäuser)
[39] Elliott R J, Krumhansl J A and Leeth P L 1974 *Rev. Mod. Phys.* **46** 465

[40] Grussbach H and Schreiber M 1993 *Phys. Rev.* B **48** 6650
[41] MacKinnon A and Kramer B 1983 *Z. Phys.* B **53** 1
[42] Economou E N, Soukoulis M and Zdetsis A D 1984 *Phys. Rev.* B **30** 1686
[43] Schreiber M and Ottomeier M 1992 *J. Phys.: Condens. Matter* **4** 1959
[44] Ono Y, Ohtsuki T and Kramer B 1989 *J. Phys. Soc. Japan* **58** 1959
[45] Mott N F and Davis E A 1979 *Electronic Processes in Non-Crystalline Materials* (Oxford: Clarendon)
[46] Efros A and Shklowskii B I 1975 *J. Phys. C: Solid State Phys.* **8** 49